An integral meshless-based approach in electromagnetic scattering

Williams L. Nicomedes
Department of Electronics Engineering, Federal University of Minas Gerais, Belo Horizonte, Brazil
Renato C. Mesquita
Department of Electrical Engineering, Federal University of Minas Gerais, Belo Horizonte, Brazil, and
Fernando J.S. Moreira
Department of Electronics Engineering, Federal University of Minas Gerais, Belo Horizonte, Brazil

Abstract

Purpose – The purpose of this paper is to solve the electromagnetic scattering problem through a new integral-based approach that uses the moving least squares (MLS) meshless method to generate its shape functions.

Design/methodology/approach – The electric field integral equation and its magnetic counterpart (MFIE) are discretized via special shape functions built numerically through the MLS procedure. This approach is applied to the particular problem concerning the scattering of a TM plane wave by an infinite conductor cylinder. An error norm is established in order to verify the quality of the obtained results.

Findings – Results show that the discretization process which employs MLS shape functions presents very good precision and fast convergence to the solution, when compared to results provided by another numerical method, the method of moments.

Originality/value – MLS shape functions occur in meshless methods intended to solve problems based on differential formulation. This paper shows that these shape functions can also be applied successfully to problems coming from an integral formulation.

Keywords Electromagnetism, Numerical analysis

Paper type Research paper

1. Introduction

In electrodynamics, particularly in its branch related to the study of high-frequency fields, it is common practice to employ the method of moments (MoM) as an aid to obtain precise numerical solutions to integral equations related to scattering phenomena (Peterson *et al.*, 1998). Meshless methods have successfully been applied as a feasible alternative to the finite element method (FEM) in static (Viana and Mesquita, 1999; Parreira *et al.*, 2006; Fonseca *et al.*, 2008) and low-frequency problems (Bottauscio *et al.*, 2006). Recently, they have also been applied to solve electromagnetic-scattering problems (Manzin and Bottauscio, 2008). In all the above applications, the weak form of the problem has been discretized using the element-free Galerkin method (Liu, 2002). In this paper, we provide another approach: we directly discretize the integral equations arising in electrodynamics.

COMPEL: The International Journal for Computation and Mathematics in Electrical and Electronic Engineering
Vol. 29 No. 6, 2010
pp. 1464-1473

0332-1649
DOI 10.1108/03321641011078535

2. The meshless approach

2.1 Presentation

The meshless approach begins by spreading nodes over the domain of the problem to be solved. Nodes are simple points and to each one a shape function is associated. Each shape function has the property of being zero over the whole domain, except in the vicinity of the corresponding node. The vicinal region in which the shape function is different from zero is the node's influence domain (Liu, 2002). The main difference between meshless methods and mesh-based methods (like the FEM) is that the element concept is not present. The shape of each influence domain is arbitrary; the only restriction is that the whole set of domains must cover the problem region entirely (i.e. without leaving holes). These influence domains can even overlap with each other. Besides that, the nodes can be distributed arbitrarily over the domain. No mesh is required.

For a given point (e.g. point $\vec{x} = X$ in Figure 1), an unknown solution u is expressed as a sum of the contributions of those nodes that influence X, i.e. nodes that extend their influence domains onto X (they are shown inside the circular-shaded region):

$$u(\vec{x}) \sim u^h(\vec{x}) = \sum_{i=1}^{N} \phi_i(\vec{x})\hat{u}_i = \Phi(\vec{x})u \tag{1}$$

where u^h is the approximated solution, N is the number of nodes whose influence domains include the point $\vec{x}$, each ϕ_i is the ith node shape function evaluated at $\vec{x}$, and $\hat{u}_i$ is the associated nodal parameter.

2.2 Constructing the shape functions

As there is no mesh to support the construction of shape functions, they are built using the moving least squares (MLS) approximation (Liu, 2002). In the MLS, u^h is expressed as:

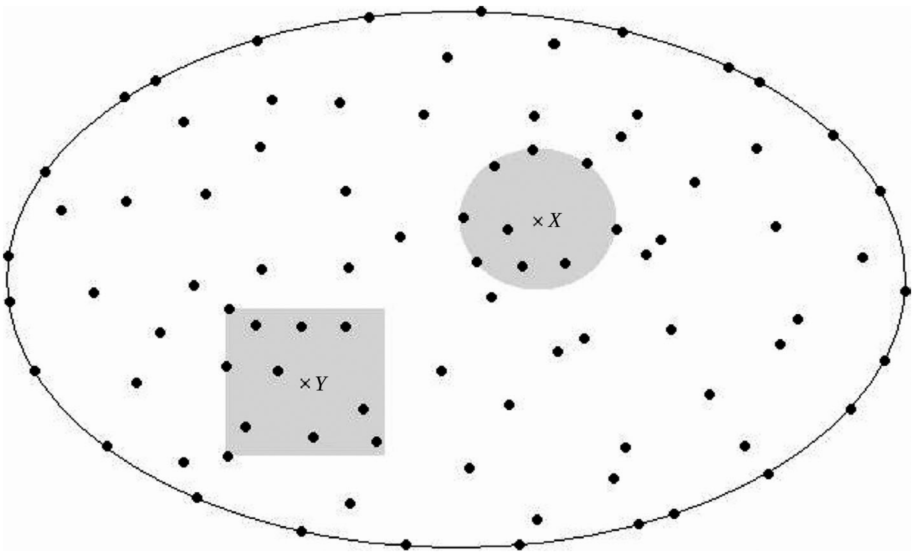

Note: Those ones that influence points X and Y are shown as belonging to regions that surround these points (shaded regions)

Figure 1. Nodes spread in a domain

$$u^h(\vec{x}) = \sum_{j=1}^{m} p_j(\vec{x})a_j(\vec{x}) = p^T(\vec{x})\alpha(\vec{x}) \tag{2}$$

where p is a monomial basis with m terms (e.g. $p(\vec{x}) = [1, x, y]$) and α is a vector of coefficients which are functions of $\vec{x}$. We then build a slightly different approximation, by requiring the monomial basis to be calculated at each node:

$$u^h(x, \vec{x}_i) = \sum_{j=1}^{m} p_j(\vec{x}_i)a_j(\vec{x}) = p^T(\vec{x}_i)a(\vec{x}) \tag{3}$$

The next step is to define a weighted functional M:

$$M = \sum_{i=1}^{N} w\left(\frac{||\vec{x} - \vec{x}_i||}{d_i}\right)\left[u^h(\vec{x}, \vec{x}_i) - \hat{u}_i\right]^2 \tag{4}$$

or:

$$M = \sum_{i=1}^{N} w\left(\frac{||\vec{x} - \vec{x}_i||}{d_i}\right)\left[\sum_{j=1}^{m} p_j(\vec{x}_i)a_j(\vec{x}) - \hat{u}_i\right]^2 \tag{5}$$

where d_i is the size of the influence domain associated to node i and w is a function with compact support centered in node i. We have chosen it to be a cubic spline (Liu, 2002):

$$w = \begin{cases} 2/3 - 4r^2 + 4r^3, & 0 \leq r \leq 0.5 \\ 4/3 - 4r + 4r^2 - 4/3r^3, & 0.5 < r \leq 1 \\ 0 & r > 1 \end{cases} \tag{6}$$

where:

$$r = \frac{||\vec{x} - \vec{x}_i||}{d_i}.$$

Looking for the coefficients a_j that minimize the functional, we impose:

$$\frac{\partial M}{\partial a} = 0 \tag{7}$$

After some matrix manipulation, we obtain:

$$a(\vec{x}) = \left[A(\vec{x})\right]^{-1}\left[B(\vec{x})\right]u \tag{8}$$

where:

$$u^T = \left[\hat{u}_1, \hat{u}_2, \ldots, \hat{u}_N\right] \tag{9}$$

$$A(\vec{x}) = P^T W(\vec{x})P \tag{10}$$

$$B(\vec{x}) = P^T W(\vec{x}) \tag{11}$$

which are given in terms of:

$$P = \begin{bmatrix} p_1(\vec{x}_1) & \cdots & p_m(\vec{x}_1) \\ \vdots & \ddots & \vdots \\ p_1(\vec{x}_N) & \cdots & p_m(\vec{x}_N) \end{bmatrix} \tag{12}$$

$$w(\vec{x}) = \begin{bmatrix} w\left(\frac{\|\vec{x}-\vec{x}_1\|}{d_1}\right) & \cdots & 0 \\ \vdots & \ddots & \vdots \\ 0 & \cdots & w\left(\frac{\|\vec{x}-\vec{x}_N\|}{d_N}\right) \end{bmatrix} \tag{13}$$

By equating the expressions(1) and (2), the shape functions calculated at $\vec{x}$ are readily available:

$$\Phi(\vec{x}) = [\phi_1(\vec{x}), \ldots, \phi_N(\vec{x})] = p^T A^{-1}(\vec{x})B(\vec{x}) \tag{14}$$

3. Scattering analysis

3.1 Integral equations

The problem to be analyzed is that of a normally incident monochromatic TM^z plane wave scattered by an infinite perfect electric conductor (PEC) cylinder. The scattered field can be evaluated after the induced surface electric current density J_s is determined. For a cylinder infinite in the z-direction, along which the current flows ($J_s \rightarrow J_z$), no quantity is dependent upon z. Hence, the problem is two-dimensional and the calculations are made only regarding the cylinder cross-section. The incident TM plane wave, coming from the left and having only the z-component is:

$$E_z^i(\vec{x}) = E_z^i(x,y) = E_0 e^{-jkx} \tag{15}$$

where E_0 is an amplitude constant and $k = (2\pi)/\lambda$ is the wave number (λ being the wavelength).

Two integral equations are cast for the numerical solution to the scattering problem. By reasoning about the electric field, from the boundary condition for the total field (incident and scattered):

$$E_z^i(\vec{x}) + E_z^s(\vec{x}) = 0 \text{ at the cylinder surface} \tag{16}$$

and from the expression for the scattered field (Peterson *et al.*, 1998):

$$E_z^s(\vec{x}) = \left(\frac{\nabla\nabla\cdot + k^2}{j\omega\varepsilon}\right) \oint J_z(\vec{x}\,')H_0^{(2)}(kR)dl' \tag{17}$$

one obtains the electric field integral equation (EFIE):

$$E_z^i(\vec{x}) = \frac{\omega\mu}{4} \oint J_z(\vec{x}')H_0^{(2)}(kR)dl' \tag{18}$$

where $\vec{x}$ and $\vec{x}\,'$ locate the observation and source points at the cylinder cross-section perimeter, respectively, $R = \|\vec{x} - \vec{x}\,'\|$, $\omega = 2\pi f$, where f is the wave frequency, ε is the permittivity of the medium, and $H_0^{(2)}$ is the zero-order Hankel function of the second type. The integral equation (18) is to be evaluated over the entire perimeter of the cross-section.

By reasoning about the magnetic field, from the boundary condition (also at the cylinder surface):

$$\hat{n} \times \left[\vec{H}^i(\vec{x}) + \vec{H}^s(\vec{x})\right] = \vec{J}_s(\vec{x}) = \hat{z}J_z(\vec{x}) \tag{19}$$

and from the expression for the scattered field (1):

$$\vec{H}^s(\vec{x}) = \nabla \times \hat{z} \oint J_z(\vec{x}')H_0^{(2)}(kR)dl' \tag{20}$$

the magnetic field integral equation (MFIE) is obtained:

$$\hat{n} \times \vec{H}^i(\vec{x}) = \hat{z}J_z(\vec{x}) - \hat{n} \times \nabla \times \hat{z} \oint J_z(\vec{x}')H_0^{(2)}(kR)dl' \tag{21}$$

In principle, both EFIE and MFIE can be used to solve for J_z. However, spurious resonant solutions may come into the scene and compromise the precision of the numerical evaluation, especially for an electrically large cylinder cross-section (Peterson *et al.*, 1998). The resonance problem can be avoided by a linear combination of equations (18) and (21):

$$CFIE = \alpha \;\; EFIE + (1 - \alpha)\eta \;\; MFIE \tag{22}$$

where α is a parameter ranging from zero to one and η is the intrinsic impedance of the exterior medium. Equation (22) is the combined field integral equation (CFIE) and α is generally set equal to 0.5 (Peterson *et al.*, 1998).

3.2 CFIE meshless numerical solution

The problem at hand consists of numerically evaluating the surface integral equation (22) in order to obtain the surface electric current J_z. Nodes are then spread along the perimeter of the cylinder cross-section (Figure 2). Figure 3 shows the shape functions for ten

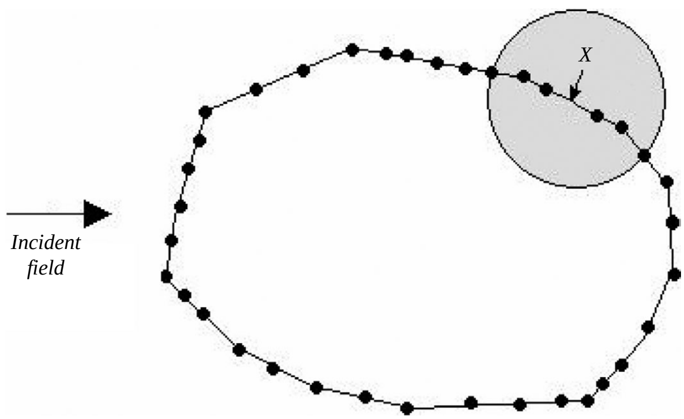

Figure 2.
Nodes at the cylinder cross-section boundary

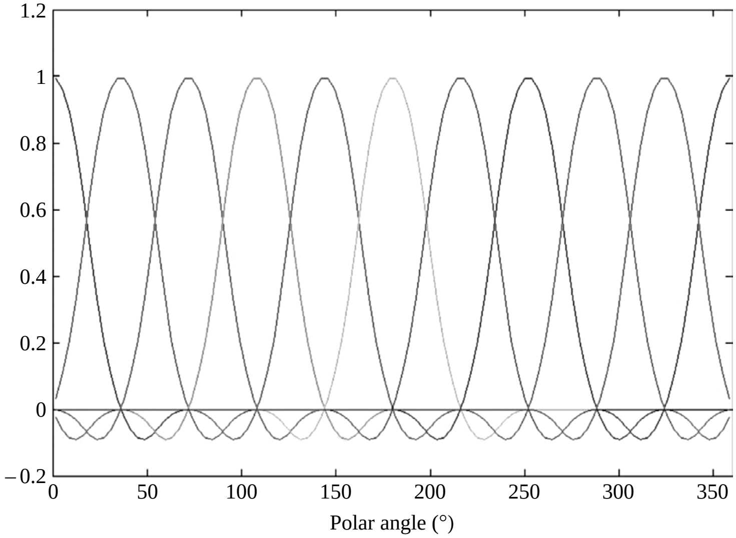

Figure 3.
A set of ten shape functions for a circular cross-section

uniformly spaced nodes distributed along the contour. Expressing the surface current as a sum of shape functions built through the MLS approximation there follows:

$$J_z(\vec{x}) = \sum_{i=1}^{N} \phi_i(\vec{x})\vec{u}_i \tag{23}$$

Taking the CFIE (equation (22)) for each observation point $\vec{x}_i$ (locus of the node i, determined by its polar angle φ_i) and applying equation (23) to represent J_z in equation (22), we get the following linear system in u:

$$\sum_{j=1}^{N} K_{ij}^{c}\widehat{u}_j = f_i^c \tag{24}$$

where:

$$K_{ij}^{c} = \alpha K_{ij}^{e} + (1-\alpha)\eta K_{ij}^{m} \tag{25}$$

$$f_i^c = \alpha f_i^e + (1-\alpha)\boldsymbol{\eta} f_i^m \tag{26}$$

$$K_{ij}^{e} = \frac{\omega\mu}{4}\oint \phi_j(\vec{x}')H_0^{(2)}(kR)dl' \tag{27}$$

$$K_{ij}^{m} = \frac{1}{2}\,\phi_j(\vec{x}_i) + \frac{jk}{4}\oint \phi_j(\vec{x}')H_1^{(2)}(kR)[\hat{n}\cdot\hat{R}]dl' \tag{28}$$

$$f_i^e = E_z^i(\vec{x}_i) \tag{29}$$

$$f_i^m = \left\{\hat{n}\times\vec{H}_i(\vec{x}_i)\right\}\cdot\hat{z} \tag{30}$$

and $H_1^{(2)}$ is the first-order Hankel function of the second type. In equations (28) and (30), the coefficients have been obtained from equation (21) after some vector manipulation. Once the $\hat{u}_i$ parameters are found, the surface current density at a given $\vec{x}$ can be determined by first finding the nodes that influence $\vec{x}$ and then applying equation (23). K^c is symmetrical, but it is not sparse. This shortcoming is due to the fact that the Hankel functions centered at a node extend their influence over the whole domain, thus making any coefficient K_{ij}^c different from zero.

4. Numerical results

In order to evaluate the convergence of the method, we have chosen the scattering of a plane wave by a circular PEC cylinder. This problem possesses analytical solution, thus providing means to study the precision of the numerical results. The scattering equations can be specialized for a circular cylinder through the use of polar coordinates (ρ, φ) to locate a point at the cylinder surface. As the radius of the cross-section is constant ($\rho = a$), the equations become functions of φ alone. Figure 4 shows the geometry of the problem.

At the cylinder surface $\rho = a$, the incident field is expressed as:

$$E_z^i(\vec{x}) = E_z^i(\vec{\rho}) = E_z^i(\rho, \varphi) = E_z^i(\varphi) = E_0 e^{-jk\alpha \cos\varphi} \tag{31}$$

In performing the plane-wave scattering analysis for a PEC cylinder with radius $\alpha = 10\lambda$ and for an incoming plane wave of unit amplitude, the number of nodes uniformly distributed over the circular perimeter was gradually increased from 10 to 600. We found that when the number of nodes is greater than 100, the solution begins to converge, when compared to the analytical solution (Balanis, 1989):

$$J_z(\vec{\rho}) = \frac{2E_0}{\pi\alpha\omega\mu} \sum_{n=-\infty}^{+\infty} j^{-n} \frac{e^{jn\varphi}}{H_n^{(2)}(k\alpha)} \tag{32}$$

where φ is the observation angle along the circular contour and $H_n^{(2)}$ is the nth-order Hankel function of the second type. Figure 5 shows the comparison between the current amplitude obtained from the meshless method (for 250 uniformly distributed nodes) and its analytical expression (32) as a function of φ. From Figure 5 one observes that both curves are almost indistinguishable.

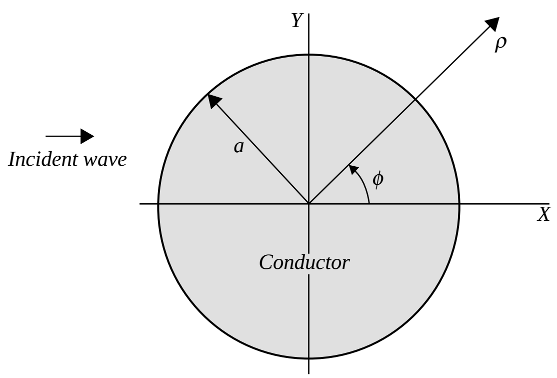

Figure 4.
The geometry of the problem: a circular cylinder cross-section

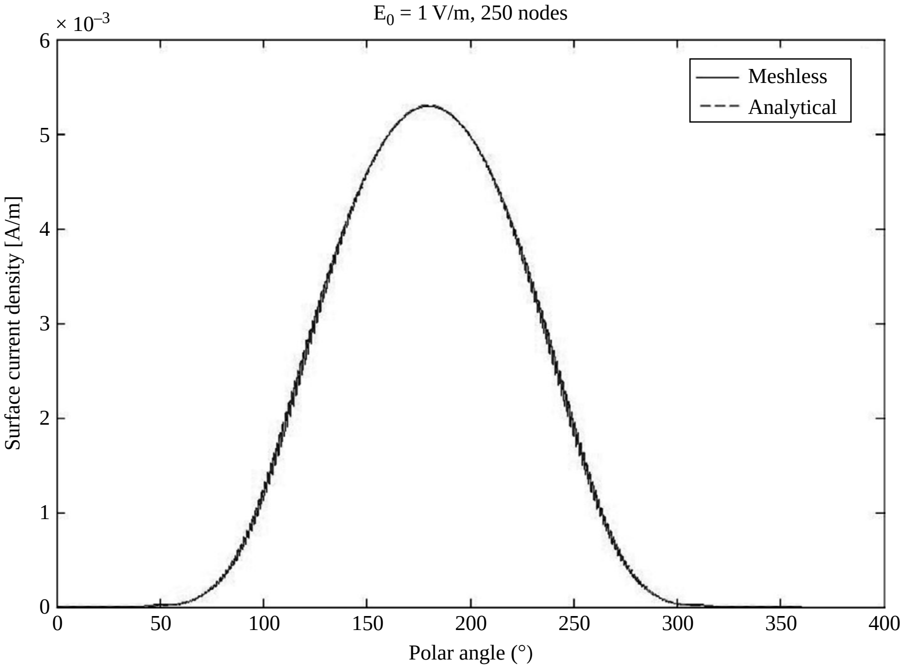

Note: 250 nodes have been spread along the contour during the analysis

Figure 5. Surface current modulus for a PEC circular cylinder, radius $\alpha = 10\lambda$

To study the numerical convergence of the proposed procedure, the following RMS norm was used as a measure of the error between the numerical and analytical solutions:

$$norm = \sqrt{\frac{1}{2\pi\alpha}\oint\left[J_{z_{Analytical}} - J_{z_{Numerical}}\right]^2 dl'} \tag{33}$$

Figure 6 shows a log-log plot of the error norm as a function of the discretization length h, where h is the distance between two consecutive nodes along the circular contour. A linear regression applied to the rectilinear portion of the graph (abscissa between 0.8 and 1.1) shows that the convergence rates are approximately 3.07 for the meshless method and 2.66 for MoM, when the CFIE is employed.

Besides that the meshless approach provides a smaller RMS error norm. Away from the cylinder internal resonances, the convergence rates for the RMS current error calculated through MoM for a flat facet mesh with pulse expansion and delta testing functions (point matching), are approximately two for the EFIE and one for MFIE alone (Davis and Warnick, 2003).

5. Conclusions

In this work, we have analyzed the plane-wave scattering by a PEC cylinder using surface integral equations numerically evaluated by a meshless-based method. As we have employed a surface integral formulation, the resulting matrix K^c is not sparse, although symmetrical. The results obtained show that the numerical solution based on

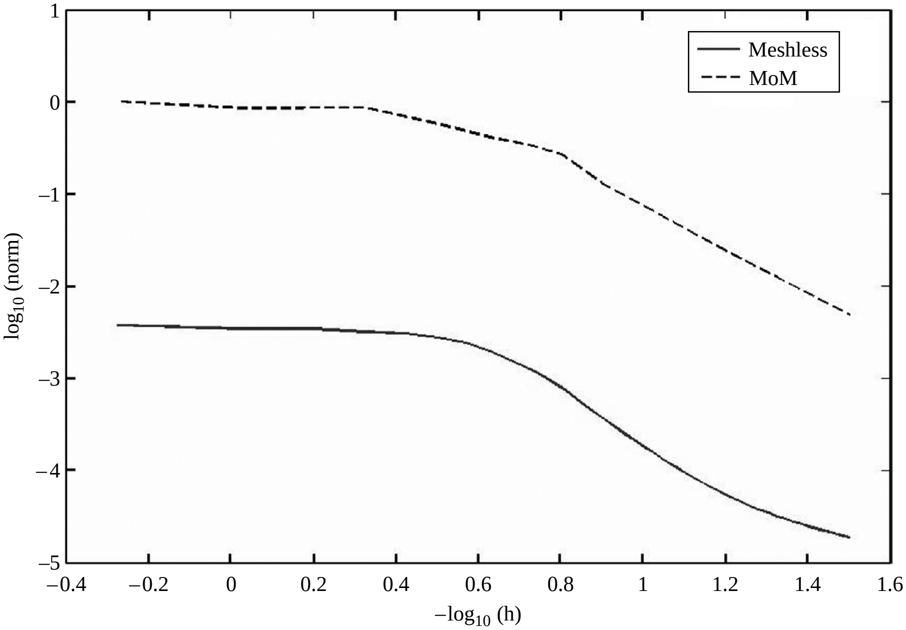

Figure 6.
Convergence of the error norm for the meshless approach and for a MoM analysis employing pulse expansion functions and point matching

a meshless approach presents very good precision and converges to the analytical solution in a satisfactory way.

References

Balanis, C. (1989), *Advanced Engineering Electromagnetics*, Wiley, New York, NY.

Bottauscio, O., Chiampi, M. and Manzin, A. (2006), "Element-free Galerkin method in eddy-current problems with ferromagnetic media", *IEEE Transactions on Magnetics*, Vol. 42 No. 5, pp. 1577-84.

Davis, C. and Warnick, K. (2003), "Convergence rates of 2D moment method solutions for the MFIE and EFIE", *IEEE Antennas and Propagation Society International Symposium, Columbus, OH, USA, June*, pp. 1080-3.

Fonseca, A.R., Viana, S.A., Silva, E.J. and Mesquita, R.C. (2008), "Imposing boundary conditions in the meshless local Petrov-Galerkin method", *IET Science Measurement & Technology*, Vol. 2, p. 387.

Liu, G. (2002), *Mesh Free Methods: Moving Beyond the Finite Element Method*, CRC Press, Boca Raton, FL.

Manzin, A. and Bottauscio, O. (2008), "Element-free Galerkin method for the analysis of electromagnetic-wave scattering", *IEEE Transactions on Magnetics*, Vol. 44 No. 6, pp. 1366-9.

Parreira, G., Silva, E., Fonseca, A. and Mesquita, R. (2006), "The element-free Galerkin method in 3-dimensional electromagnetic problems", *IEEE Transactions on Magnetics*, Vol. 42 No. 4, pp. 711-4.

Peterson, A., Ray, S. and Mittra, R. (1998), *Computational Methods for Electromagnetics*, IEEE Press, Piscataway, NJ.

Viana, S.A. and Mesquita, R.C. (1999), "Moving least squares reproducing kernel for electromagnetic field computation", *IEEE Transactions on Magnetics*, Vol. 35 No. 3, pp. 1372-5.

About the authors

Williams L. Nicomedes received his Bachelor's degree in Electrical Engineering from the Federal University of Minas Gerais (UFMG) in 2008. Currently, he is working towards a Master's degree in Electrical Engineering under Fernando J.S. Moreira and Renato C. Mesquita at UFMG. He is interested in numerical methods and applied mathematics. Williams L. Nicomedes is the corresponding author and can be contacted at: wlnicomedes@yahoo.com.br

Renato C. Mesquita is a Professor at Electrical Engineering Department, Federal University of Minas Gerais, Brazil. He received his BE and MSc degrees from the Federal University of Minas Gerais, 1982 and 1987, and his PhD from the Federal University of Santa Catarina, Brazil, 1990. His main research interest is in the area of electromagnetic field computation.

Fernando J.S. Moreira received the BS and MS degrees in Electrical Engineering from the Catholic University, Rio de Janeiro, Brazil, in 1989 and 1992, respectively, and the PhD degree in Electrical Engineering from the University of Southern California in 1997. Since 1998, he has been with the Department of Electronics Engineering of the Federal University of Minas Gerais, Brazil, where he is currently an Associate Professor. His research interests are in the areas of electromagnetics, antennas and propagation. He has authored or co-authored over 100 journal and conference papers in these areas. He is a member of Eta Kappa Nu, IEEE Antennas and Propagation Society, and the Brazilian Microwave and Optoelectronics Society.